ChemInform Abstract: Hydrothermal and Postsynthesis Surface Modification of Cubic, MCM-48, and Ultralarge Pore SBA15 Mesoporous Silica with Titanium

ARTICLE *in* CHEMINFORM · JULY 2010

Impact Factor: 0.74 · DOI: 10.1002/chin.200029217

4 AUTHORS, INCLUDING:

Stephen O'Brien

City College of New York

126 PUBLICATIONS **7,688** CITATIONS

Articles

Hydrothermal and Postsynthesis Surface Modification of Cubic, MCM-48, and Ultralarge Pore SBA-15 Mesoporous Silica with Titanium

Mark S. Morey,[†] Stephen O'Brien,[†] Stephan Schwarz,[‡] and Galen D. Stucky*[,†]

Department of Chemistry and Materials Research Laboratory, University of California, Santa Barbara, California 93106 and DuPont Experimental Station, Wilmington, Delaware 19880-0262

Received March 22, 1999. Revised Manuscript Received January 27, 2000

We describe the introduction of titanium centers to cubic MCM-48 and SBA-15 mesoporous silica by hydrothermal and postsynthetic grafting techniques. MCM-48 was hydrothermally prepared with a gemini surfactant that favors the cubic phase and leads to a high degree of long-range pore ordering. This phase was chosen due to its high surface area (1100−1300 m^2/g) and its three-dimensional, bicontinuous pore array. SBA-15, synthesized with a block copolymer template under acidic conditions, has a surface area from 600 to 900 m^2/g and an average pore diameter of 69 Å, compared to 24−27 Å for MCM-48. Alkoxide precursors of titanium were used to prepare samples of Ti-MCM-48 and Ti-SBA-15. We have detailed the bulk and molecular structure of both the silica framework and the local bonding environment of the titanium ions within each matrix. X-ray powder diffraction and nitrogen adsorption shows the pore structure is maintained despite some shrinkage of the pore diameter at high Ti loadings by grafting methods. UV−visible and Raman spectroscopy indicate that grafting produces the least amount of Ti−O−Ti bonds and instead favors isolated tetrahedral and octahedral titanium centers. High-resolution photoacoustic FTIR spectra demonstrated the presence of intermediate range order within the silicate walls of MCM-48, established the consumption of surface silanols to form Si−O−Ti bonds by grafting, and resolved the characteristic IR absorbance at 960 cm^{-1}, occurring in titanium silicates, into two components. All three spectroscopic techniques, including in situ Raman, reveal the reactive intermediates formed when the materials are contacted with hydrogen peroxide.

Introduction

Silica-based, mesoporous materials have attracted intense interest due to their high potential as supports for catalytic applications. Of these materials, the cubic MCM-48 phase possesses a unique configuration of a bicontinuous, three-dimensional array of pores.[1,2] Ordered mesoporous silica with uniform pore diameters in the range 15−300 Å can be synthesized via solution or hydrothermal methods from silica precusors and an appropriate organic template, with subsequent calcination to produce accessible pore volumes. MCM-48,[3] with surface areas 1000−1450 m^2/g, and pore volumes of 0.8−1.1 cm^3/g, can be synthesized from standard ($C_nH_{2n-1}N(CH_3)_3^+$, where $8 \leq n \leq 20$) or gemini ($C_nH_{2n-1}N(CH_3)_2(CH_2)_{12}N(CH_3)_2C_nH_{2n-1}^{2+}$, where $16 \leq n \leq 22$) cationic alkylammonium surfactants, whereas SBA-15[4,5] is obtained using block copolymers in an acidic medium. SBA-15 materials exhibit surface areas from 600 to 1000 m^2/g and pore volumes 0.6−1.3 cm^3/g, determined by nitrogen adsorption analysis. The primary difference as a support matrix is the large pore diameter range for SBA-15 of 50−300 Å versus 20−30 Å for MCM-48. The resulting surface within the pores is adorned with a high density of silanol groups which then provide convenient, reactive sites for advantageous modification through functionalization. By using both hydrothermal and postsynthesis grafting to incorporate titanium into the mesoporous silica, we combine the catalytic activity of Ti and the high surface area of the support to produce mesoporous materials which are accessible to large molecules(>10 Å kinetic diameter)

[†] University of California.
[‡] DuPont Experimental Station.

(1) Kresge, C. T.; Leonowicz, M. E.; Roth, W. J.; Vartuli, J. C.; Beck, J. S. *Nature* **1992**, *359*, 710.
(2) Beck, J. S.; Vartuli, J. C.; Roth, W. J.; Leonowicz, M. E.; Kresge, C. T.; Schmitt, K. D.; Chu, C. T. W.; Olson, D. H.; Sheppard, E. W.; McCullen, S. B.; Higgins, J. B.; Schlenker, J. L. *J. Am. Chem. Soc.* **1992**, *114*, 10834.
(3) Huo, Q. S.; Margolese, D. I.; Stucky, G. D. *Chem. Mater.* **1996**, *8*, 1147.
(4) Zhao, D.; Feng, J.; Huo, Q.; Melosh, N.; Fredrickson, G. H.; Chmelka, B. F.; Stucky, G. D. *Science* **1998**, *279*, 548.
(5) Zhao, D. Y.; Huo, Q. S.; Feng, J. L.; Chmelka, B. F.; Stucky, G. D. *J. Am. Chem. Soc.* **1998**, *120*, 6024.

10.1021/cm9901663 CCC: $19.00
Published on Web 03/17/2000

for fine chemical catalytic applications.

Examples of Ti hydrothermally incorporated into zeolites include TS-1,[6,7] TS-2,[8] and Beta-Ti,[9] with pore apertures of 5.4 Å, 5.3 × 5.4 Å, and 6.4 × 7.4 Å, respectively. These materials have been successful in the epoxidation of alkenes but are limited to molecules small enough to fit into their pores. By using mesoporous silica with primarily amorphous walls, incorporation of large transition metal cations should be easier than in the case of crystalline zeolites. Of the numerous attempts to incorporate transition metals into mesoporous silica by hydrothermal or postsynthesis treatment methods, those made with titanium appear most promising for catalytic applications.[10−16] With the exception of Mn[17] and Ti-MCM-48,[14,18,19] these efforts have focused on the hexagonal phase, MCM-41, consisting of a one-dimensional array of pores which could be clogged during use. Generally, the incorporation of large transition metal cations into the silica lattice often results in lowered crystallinity and surface area of the products and potentially compromises structural durability.

The cubic, MCM-48 phase features the same high surface area as MCM-41 but possesses a three-dimensional array of pores within a 20−30 Å diameter range. SBA-15 has a similar hexagonal pore array as MCM-41 but posesses thicker walls and a larger pore diameter range. We reported previously the synthesis of Ti-MCM-48 by the hydrothermal process.[14] This method produced a durable silicate framework with up to 3.5 atomic % Ti in the walls and an absence of extraframework, crystalline TiO_2 clusters. Since hydrothermal methods produce some Ti sites within the walls that are sterically inaccessible to passing molecules, a second method, consisting of grafting Ti directly to the silica MCM-48 and SBA-15 lattices via surface silanol groups will be presented and compared spectroscopically to the hydrothermally prepared Ti-MCM-48. To form covalent bonds to the silica surface, water-sensitive metal alkoxides were employed, instead of evaporating aqueous solutions onto the support by the incipient wetness technique. Using this approach, we reported the formation of isolated $O{=}VO_{3/2}$ centers on the interior pore surface of MCM-48 by reaction with a vanadium isopropoxide/hexane solution.[15] Similarly, Maschmeyer et al. described the decomposition of titanocene derivatives on MCM-41, yielding an effective epoxidation catalyst.[20] More recently, Aronson et al. used $TiCl_4$ in hexane to graft titania clusters within the pores of MCM-41 which was active in the photodegradation of rhodamine-6G.[21] To facilitate the generation of isolated titanium−oxo species on the surface of MCM-48 and SBA-15, we chose titanium isopropoxide in hexane under inert atmospheric conditions. This approach combines the high surface area and durable, silica mesoporous support with catalytically active, titanium centers to produce a material with the maximum number of active sites per titanium atom.

As we previously reported, supported and hydrothermally incorporated Ti in cubic, mesoporous silica frameworks are active biomimics for the vanadium bromoperoxidase enzyme catalyst for halogenating large organic substrates at neutral pH.[19] This particular enzyme plays a key role in the biosynthesis of halogenated marine natural products with pharmacological activity.[22] These results are significant since the Ti/MCM-48 material functions under conditions closely resembling ambient environment for the enzyme. Many attempts have been made to mimic the behavior of this enzyme in the form of various oxo−metal anions in solution. Unfortunately, each of these entries work only under extreme acidic conditions (>1 M) which are nowhere near the neutral pH system of the enzyme in the ocean environment.

Here we report the combination of UV−visible, Raman, and photoacoustic (PAS) FTIR spectroscopy to elucidate the local bonding environments found in Ti-MCM-48 made hydrothermally and Ti-MCM-48 and Ti-SBA-15 prepared by postsynthetic methods. This information about the coordination sphere of the titanium atoms with respect to both the framework and surrounding ligands yielded insight into the nature of the species responsible for the peroxidative bromination activity. Additionally, we will discuss the assignment of the IR absorption at 960 cm^{-1}, which is often reported in metal-substituted silicates and is the subject of considerable debate. Materials were made by both techniques at varying titanium concentrations and conditions to determine the effect on the titanium bonding environment and interaction with hydrogen peroxide.

Experimental Section

Materials. *N*,*N*-Dimethyloctadecylamine (95%, Pfaltz and Bauer), 1,12-dibromododecane (98%, Aldrich), pluronic P123 block copolymer (BASF), acetone (Fisher), tetraethyl orthosilicate (Fluka), cetylbenzyl dimethylammonium chloride CB-DAC (Kodak), titanium isopropoxide (97%, Gelest), tetramethylammonium hydroxide (25 wt % in water, Aldrich), titanium isopropoxy (triethanolaminato) (80% in isopropyl alcohol, Tyzor, DuPont), and all other reagents were used as received. Hexane (Aldrich) was distilled from potassium.

Synthesis[23] of $[C_{18}H_{37}(CH_3)_2N\text{-}C_{12}H_{24}\text{-}N(CH_3)_2C_{18}H_{37}]Br_2$. This particular "gemini-type" surfactant to be referred to as 18-12-18, was chosen as a template because it favors the

(6) Taramasso, M.; Perego, G.; Notari, B. US Patent 4,410,501, 1983.
(7) Clerici, M. G.; Ingallina, P. *J. Catal.* **1993**, *140*, 71.
(8) Reddy, J. S.; Sivasanker, S.; Ratnasamy, P. *J. Mol. Catal.* **1992**, *71*, 373.
(9) Camblor, M. A.; Corma, A.; Martinez, A.; Perezpariente, J. *J. Chem. Soc., Chem. Commun.* **1992**, 589.
(10) Corma, A.; Navarro, M. T.; Pérez-Pariente, J.; Sànchez, F. *J. Chem. Soc., Chem. Commun.* **1994**, 147.
(11) Tanev, P. T.; Chibwe, M.; Pinnavaia, T. J. *Nature* **1994**, *368*, 321.
(12) Yuan, Z. Y.; Liu, S. Q.; Chen, T. H.; Wang, J. Z.; Li, H. X. **1995**, *J. Chem. Soc., Chem. Commun.*, 973.
(13) Gontier, S.; Tuel, A. *Zeolites* **1995**, *15*, 601.
(14) Morey, M.; Davidson, A.; Stucky, G. *Microporous Mater.* **1996**, *6*, 99.
(15) Morey, M.; Davidson, A.; Eckert, H.; Stucky, G. *Chem. Mater.* **1996**, *8*, 486.
(16) Chen, L. Y.; Chuah, G. K.; Jaenicke, S. *Catal. Lett.* **1998**, *50*, 107.
(17) Zhao, D. Y.; Goldfarb, D. *J. Chem. Soc., Chem. Commun.* **1995**, 875.
(18) Koyano, K. A.; Tatsumi, T. *J. Chem. Soc., Chem. Commun.* **1996**, 145.
(19) Walker, J. V.; Morey, M.; Carlsson, H.; Davidson, A.; Stucky, G. D.; Buttler, A. *J. Am. Chem. Soc.* **1997**, *119*, 6921.
(20) Maschmeyer, T.; Rey, F.; Sankar, G.; Thomas, J. M. *Nature* **1995**, *378*, 159.
(21) Aronson, B. J.; Blanford, C. F.; Stein, A. *Chem. Mater.* **1997**, *9*, 2842.
(22) Buttler, A.; Walker, J. V. *Chem. Rev.* **1993**, *93*, 1937.

formation of the MCM-48 mesophase and yields a superior product compared to the standard cetyltrimethyammonium bromide.[3] A total of 12 g (36.6 mmol) of 1,12-dibromododecane and 25 g (83.9 mmol) of *N*,*N*-dimethyl octadecylamine were refluxed at a soft boil in 60 g of ethanol for 4 days. A 15% excess of *N*,*N*-dimethyloctadecylamine was used to ensure disubstitution of the 1,12-dibromododecane. The resulting brown/orange liquid was allowed to cool and then filtered and recrystallized 4 times from pure acetone or acetyl acetate/chloroform. The yield was 80% based on 1,12-dibromododecane.

Synthesis of Siliceous MCM-48 with 18-12-18. A typical synthesis involves dissolving 1.23 g (1.33 mmol) of 18-12-18 in 60 g (3.33 mmol) of deionized water with heating to 60 °C. To this solution was added 7.5 g (15 mmol) of 2 M TMAOH followed by 5.79 g (27.8 mmol) of tetraethyl orthosilicate (TEOS), bringing the pH to about 13. The solution was stirred for 2 h and then placed in a Teflon bottle and heated to 100 °C for 11 days. The crystal phase of the resulting white powder collected by vacuum filtration was confirmed by X-ray powder diffraction to be cubic ($Ia\bar{3}d$). The material was then returned to the oven with 40 mL of H_2O (~1 g/20 mL of H_2O) for an additional 11 days to improve crystallinity. This second treatment yields a well-ordered product that is more durable to calcination than materials heated for much shorter times. The final product was filtered, washed with water followed by methanol and then calcined at 550 °C for 6 h in N_2 then air to remove the surfactant. The yield was ~72% based on TEOS (Si).

Synthesis of Siliceous MCM-48 with CBDAC. As with 18-12-18, CBDAC possesses a large headgroup which also favors the MCM-48 mesophase and is easier to scale-up the recipe for larger batches.[15] By using the same approach as above, 7.88 g (19 mmol) of CBDAC was dissolved in 171 g (9.5 mol) deionized water with heating. The pH was raised to ~13 with 10 g (20 mmol) of 2 M TMAOH followed by 10.42 g (50 mmol) of TEOS. This solution was rapidly stirred for 2 h and then transferred to a 500-mL Teflon bottle and placed in a 100 °C oven for 15 days. The product was filtered and then returned to the 100 °C oven for an additional 8 days to give a more crystalline product as before. The final product was filtered, washed with water followed by methanol, and then calcined at 550 °C for 6 h to remove the surfactant. The yield was ~80% based on TEOS (Si).

Synthesis of Ti-MCM-48 with 18-12-18. As reported previously,[14] 0.22 g (0.7 mmol) of titanium isopropoxy (triethanolaminato) was added to the above recipe immediately following the addition of TEOS. This particular chelated titanium source was chosen because its rate of hydrolysis is slower than titanium isopropoxide and similar to that of TEOS, thus avoiding a heterogeneous precipitation of TiO_2 followed by SiO_2. Samples made hydrothermally will be referred to as Ti-MCM-48H. Elemental analysis (Galbraith Laboratories, Knoxville, TN) showed the Ti/Si ratio in the final product to be 1:28.

Synthesis of Ti-MCM-48 with CBDAC. By using the same procedure for the synthesis of pure silica MCM-48 with CBDAC, 0.73 g (2.27 mmol) of titanium isopropoxy(triethanolaminato)−isopropyl alcohol was added immediately following the addition of TEOS (50 mmol) to give a Ti/Si ratio of 1/22 in the gel. Elemental analysis showed the Ti/Si ratio in the final product to be 1:25.

Grafting of Ti on Dehydrated, Siliceous MCM-48. Upon calcination, internal surface silanols are generated by replacing surfactant cations with protons in the terminal $Si-O^-$ groups. Titanium isopropoxide was then used to graft titanium to the surface of calcined MCM-48 via the surface silanols. Grafted samples will be referred to as Ti-MCM-48G. This titanium source was chosen over $TiCl_4$ to avoid damage to the framework from the corrosive HCl byproduct, as previously observed by XRD of Ti/MCM-41.[21]

To remove any physisorbed water from the calcined MCM-48 before grafting Ti, a weighed sample of the material (made with either 18-12-18 or CBDAC) was dehydrated at 300 °C for 3 h under flowing O_2 or house vacuum in a tube furnace. Great care was taken to avoid the introduction of moisture which could lead to the precipitation of TiO_2 within the pores.[24] After the sealed tube was placed in a glovebag filled with argon, the sample was mixed with a solution of titanium isopropoxide in anhydrous hexane corresponding to the desired atomic % Ti. The mixture stood for 1 h and was then filtered and washed (3 × 15 mL) with anhydrous hexane. The grafted material was returned to the tube furnace and calcined at 400 °C for 4 h in O_2 to convert unrected alkoxide ligands into Ti−OH groups, and to remove residual isopropyl alcohol and hexane. The same procedure was used to produce a sample using excess titanium isopropoxide to determine the maximum coverage possible. Elemental analysis showed the Ti/Si ratio in the 5% Ti product to be 1:32, 1:10.1 in the 10% sample and 1:5.6 (18 wt %) in the XS-Ti sample.

Synthesis of SBA-15 with PEO-PPO-PEO. SBA-15 was synthesized according to methods described previously,[4] using the amphiphilic triblock copolymer poly(ethylene oxide)-poly(propylene oxide)-poly(ethylene oxide). Large pore mesoporous silica possessing the *p*6*mm* hexagonal morphology is obtained from an aqueous acidic solution of the triblock copolymer, composition $EO_{20}PO_{70}EO_{20}$, and tetraethyl orthosilicate (TEOS). The mixture is stirred at 25 °C and then heated to 100 °C in a Teflon bottle. The chemical composition was 2 g copolymer: 0.021 mol TEOS:0.12 mol HCl:3.33 mol H_2O. To remove the copolymer, the as-synthesized sample was calcined in air to 400 °C for 4 h.

Grafting of Ti on Dehydrated SBA-15. SBA-15 (200 mg) was dehydrated at 300 °C under high vacuum (10^{-5} Torr) for 6 h and then transferred to a Schlenk line and placed under argon. A total of 0.06 mL (0.22 mmol) titanium isopropoxide $Ti(OiPr)_4$ in 15 mL of dry hexane was added through the septum. The grafted sample was washed with three portions of dry hexane and dried under vacuum. The sample was not filtered, and it was assumed that all titanium isopropoxide reacted with the SBA-15 surface. Calcination was at 400 °C for 4 h in O_2. Elemental analysis of the product showed 6 wt % titanium, corresponding to a Ti/Si ratio of 1:22. The grafted sample was denoted Ti-SBA-15G.

Instrumentation

X-ray powder diffraction patterns were obtained on a Scintag PADX diffractometer using Cu Kα radiation with a liquid nitrogen cooled solid-state detector at 45 kV and 40 mA. Nitrogen absorption/desorption isotherms were measured on a Micromeritics ASAP 2000 apparatus. All samples were outgassed initially at room temperature then at 150−200 °C until a pressure <1 μTorr was achieved.

The UV−visible spectra were measured with a Cary 5 UV−vis−NIR spectrophotometer equipped with the Varian diffuse reflectance attachment. The halon/quartz cover slide that covers the sample was subtracted out of every scan. The Teflon integrating sphere that was used has very low absorbance in the range of our scans, and hence has negligible influence on our results. Titanium-grafted materials were contacted with a dilute 5% solution of H_2O_2 and run as a paste. The standard Kubelka Munk function was used to analyze the data.[25]

The mid-infrared spectra presented have been collected on the Nicolet Magna 850 FT-IR spectrometer by the coaddition of 150 scans at a 4 cm^{-1} resolution, using an MTEC photoacoustic detector and ultrapure He as a gas vector. Photoacoustic detection allows pure samples to be run nondestructively. Peroxide interaction studies were run on dried samples after contact with 10% aqueous solutions of hydrogen peroxide.

Raman spectra were measured with a Nicolet FT-Raman accessory, connected to a Magna 850 spectrometer, using a $Nd:YVO_4$ excitation laser with a 1064 nm excitation source. The spectra were recorded at room temperature, by the coaddition of 400 scans at a 2 cm^{-1} resolution. Peroxide

(23) Zana, R.; Benrraou, M.; Rueff, R. *Langmuir* **1991**, *7*, 1072.
(24) Srinivasan, S.; Datye, A. K.; Smith, M. H.; Peden, C. H. F. *J. Catal.* **1994**, *145*, 565.
(25) Kubelka, P.; Munk, F. *Z. Tech. Phys.* **1931**, *12*, 593.

Table 1. Preparation and Physicochemical Properties of MCM-48 (Prepared with CBDAC), Ti-MCM-48H (Ti Incorporated via Hydrothemral Methods, with 18-12-18 Surfactant), Ti-MCM48G (5% Ti Grafted on MCM-48 Made with CBDAC), SBA-15, Ti−SBA-15G (Ti Grafted)[a]

sample	*d* spacing (Å)	lattice parameter (Å)	BET surface area (m^2/g)	pore volume (cc/g)	pore diamter (Å)
MCM-48	33.7 (d_{211})	83.1[b]	1128	0.84	27.2[d]
Ti-MCM-48H	33.0 (d_{211})	81.5[b]	1296	1.03	26.6[d]
Ti-MCM-48G	33.5 (d_{211})	83.0[b]	1093	0.75	26.0[d]
SBA-15	95.7 (d_{100})	110.5[c]	696	0.87	69[e]
Ti-SBA-15G	92.2 (d_{100})	106.5[c]	518	0.68	63[e]

[a] The lattice parameter, *a*, was calculated from XRD; pore size distributions and surface areas were determined from N_2 adsorption−desorption experiments. [b] $a = d\sqrt{6}$. [c] $a = 2d_{100}/\sqrt{3}$. [d] Determined from BJH adsorption. [e] Determined from BdB adsorption.

interactions were measured in situ, by immersing the sample in a 1% hydrogen peroxide solution inside a quartz capillary.

Results and Discussion

Bulk Characterization by XRD and Nitrogen Adsorption. Bulk structural characterization by XRD of a pure silica MCM-48 support grafted with various amounts of titanium (Figure 1c−g) confirms that the structure is maintained upon incorporation of Ti by the grafting technique. Reflections in all diffractograms occur below $2\theta = 10°$ and index to the $Ia\bar{3}d$ space group, indicative of the MCM-48 mesophase.[1] The intensity and resolution of the reflections in the materials is based solely on the degree of ordering of the three-dimensional pore array, and arises from the electron density gradient between the walls and the pores. Upon calcination, the peak intensities routinely increase as the surfactant within the pores can no longer scatter X-ray photons. No higher order reflections are seen, indicating the absence of bulk (>1000 Å particle size) anatase. The blank shown in Figure 1c,d was made with the surfactant CBDAC and features over 13 reflections, which is a minimal requirement for high quality MCM-48 products. Subsequent grafting with titanium yields samples with little degradation in their diffractograms, even at the synthetic limit of this technique Figure 1e−g. Hydrothermal incorporation of Ti into MCM-48 gives a material with a similar diffractogram in terms of the number of diffraction peaks Figure 1h. However, the resolution of the peaks are decreased by a factor of 2 compared to those of the pure silica sample which could be due to smaller particle size. Upon calcination of both Ti-MCM-48 and the blank, XRD peaks increase in intensity due to an absence of scattering from the surfactant(18-12-18). The peaks also shift to lower *d* spacing as the surfactant is removed and the material undergoes further condensation and constriction of the pores.

Consistent with previous studies, all MCM-48 samples analyzed by nitrogen adsorption methods exhibited high surface areas in the range of 1000−1300 m^2/g, pore diameters from 24 to 27 Å and no observable hysteresis. Little difference was observed between pure silica MCM-48 and those containing titanium by hydrothermal methods. The results are shown in Table 1. As in the case of grafted vanadium,[15] higher titanium loadings showed an expected decrease in pore diameter and surface area. All samples possessed narrow pore size distributions (∼5 Å, fwhm) even at 18 atomic % Ti loadings, indicating an even coverage of titanium centers and a lack of pore constriction by TiO_2 clusters.

X-ray powder diffraction analysis of the SBA-15 samples showed Bragg reflections in the 2θ range 0.10−2.00 and are shown in Figure 1a,b. The reflections could be indexed to a hexagonal unit cell, $a = 110.5$ Å ($2d_{100}/\sqrt{3}$) in the case of SBA-15 and $a = 106.5$ Å for Ti-SBA-15G, and indicated a lattice contraction of ∼4%. At the relatively low calcination temperatures a large contraction of the pores would not be anticipated. The retention of the unit cell does however support highly stable nature of the material. Nitrogen adsorption isotherms of SBA-15 and Ti-SBA-15G are shown in Figure 2a,b together with Broekhoff de Boer (BdB) estimates of the pore diameter. The Broekhoff de Boer method of pore size analysis[26,27] has been shown to be a suitable alternative to the more standard Barrett−Joyner−Halenda (BJH) method[28] for materials that possess well-ordered cylindrical shaped pores in the mesoporous size regime.[29,30] Pore size distributions from the two methods

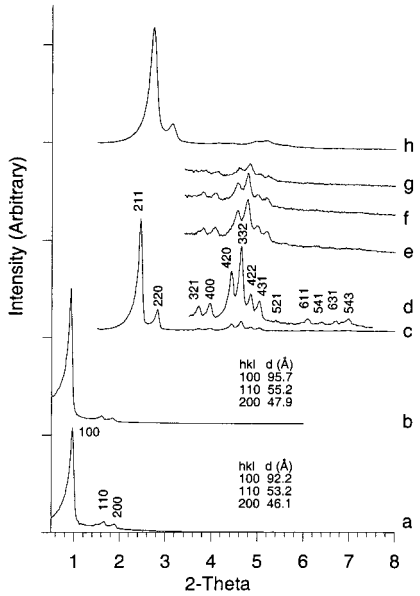

Figure 1. X-ray powder diffraction pattern of (a) SBA-15 grafted with 6% titanium, (b) pure silica, calcined SBA-15, (c) pure silica MCM-48, (d) detail, (e) MCM-48 grafted with 5% Ti, (f) 10% Ti, and (g) 17.5 atomic % Ti, (h) calcined Ti-MCM-48H.

(26) Broekhoff, J. C. P.; de Boer, J. H. *J. Catal.* **1967**, *9*, 8.
(27) Broekhoff, J. C. P.; de Boer, J. H. *J. Catal.* **1967**, *10*, 377.
(28) Barrett, E. P.; Joyner, L. G.; Halenda, P. P. *J. Am. Chem. Soc.* **1951**, *73*, 373.
(29) Schmidt-Winkel, P.; Lukens, W. W.; Zhao, D. Y.; Yang, P. D.; Chmelka, B. F.; Stucky, G. D. *J. Am. Chem. Soc.* **1999**, *121*, 254.
(30) Lukens Jr., W. W.; Zhao, D.; Schmidt-Winkel, P.; Feng, J.; Stucky, G. D. *Langmuir* **1999**, *15*, 5403. While the large amount of gas adsorbed at low relative pressure may appear to be caused by adsorption in micropores, this is not the case. As shown by the standard absorption plot, these materials have little microporosity, and the large amount of gas adsorbed at low pressures is simply due to multilayer adsorption on these large specific surface area materials.

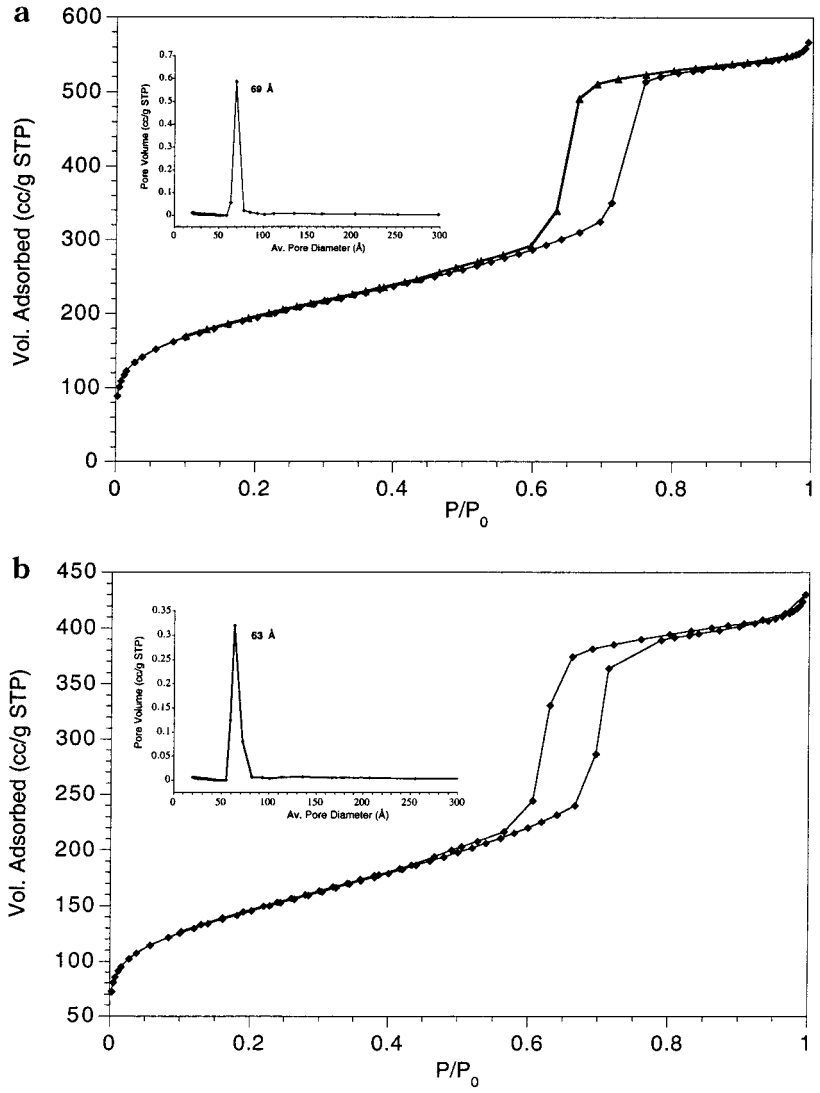

Figure 2. Nitrogen adsorption isotherms of (a) SBA-15 and (b) Ti−SBA-15G. Inset: pore size distributions determined from Broekhoff de Boer analysis.

were 52 Å (BJH) and 69 Å (BdB) for SBA-15, and 51 Å (BJH) and 63 Å (BdB) for Ti-SBA-15G. The reduction in size is markedly reflected in the BET calculated surface area, which showed a reduction of ∼25% (Table 1). The observation of the decreased surface area may be an indication of the formation of TiO_2 clusters within the pores.

To test the durability of the mesoporous materials at high temperatures or in water, samples were first heated to 800 °C overnight in static air. After heat treatment, XRD gave diffraction patterns similar to but less resolved than samples calcined to the standard 500−550 °C, illustrating good thermal stability for both hydrothermal and grafted materials. The unit cells of pure silica MCM-48 and Ti-MCM-48H undergo an average shrinkage of 45% while as the grafted material shrinks by ∼40% from the uncalcined state. The smaller degree of shrinkage for the grafted material could be due to the capping of the surface silanols by Ti which would prevent further condensation. After heating to 800 °C, the unit cells of SBA-15 and Ti-SBA-15 contracted by ∼10%. Despite the decrease in XRD peak intensity, all 800 °C calcined materials retain much of their high surface area, pore volume, and pore diameter. BET data indicates that the pore diameter shrinkage associated with Ti−MCM-48G is much less than for the blank or hydrothermal materials giving further evidence for the proposed capping effect. While the degree of titanium solubilization and deactivation in more oxidizing hydrogen peroxide solutions is uncertain, our initial study demonstrated materials heat treated to 800 °C in the above fashion were found to show superior durability and no loss of reactivity after soaking in a buffered solution for 24 h.[19]

UV−Visible Spectroscopy. After confirming that the bulk structure is maintained upon introduction of titanium by both methods mentioned, UV−vis, FTIR, and Raman spectroscopies were applied to establish the constituents of the local Ti environment. The UV−vis spectra for Ti-MCM-48H and TiO_2 calcined to 550 °C are shown in Figure 3b,c. Titania was prepared by hydrolyzing titanium isopropoxide in water and then heating with the same routine as in the complete synthesis of mesoporous silica. As expected, the anatase phase of titania was predominant under these conditions, as determined by XRD. All spectral features are due to ligand to metal charge transfers between the O^{2-} ligand and the titanium(IV) ion. No absorptions arise from silica, which is transparent in this region exemplified by the UV−visible spectrum of SBA-15 (Figure 3a).

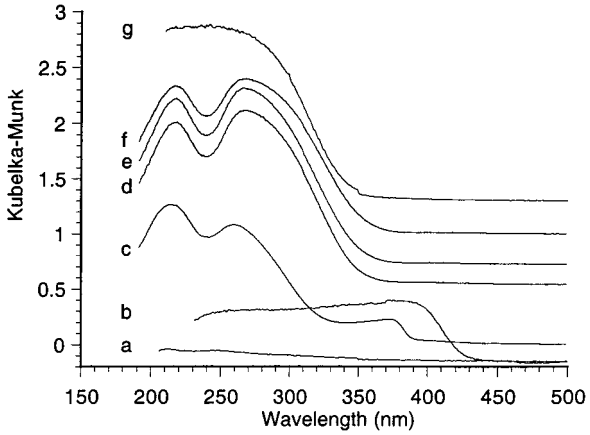

Figure 3. UV−visible spectra of (a) pure silica SBA-15, (b) TiO_2 (anatase), (c) hydrothermal Ti-MCM48, (d) 5%, (e) 10%, and (f) 17.5 atomic % titanium grafted on MCM-48, and (g) 6% titanium grafted on SBA-15.

The spectrum of anatase exhibits a broad absorption with an absorption edge at about 430 nm. The Ti-MCM-48H product features two main absorptions at 213 and 259 nm with a smaller, emerging peak at 375 nm. The first two peaks can be assigned to isolated tetrahedral (T_d) and octahedral (O_h) titanium species respectively, present within the walls or near the surface.[31−33] The third small peak at a longer wavelength of 374 nm is due to Ti in an octahedral environment participating in Ti−O−Ti bonds as part of small TiO_2 regions. The small size of these TiO_2 regions can be inferred from the blue shift in absorption edge of the Ti-MCM-48H sample versus anatase. These particles could be either extraframework or heterogeneous regions within the walls caused by incomplete mixing during synthesis and are amorphous due to the absence of diffraction in XRD and scattering in RAMAN (shown later).

The UV−visible spectrum of Ti-SBA-15G in Figure 3g shows a broad adsorption in the region starting below 360 nm. While it shows no signs of bulk titania inhomogeneities, it lacks the resolution of distinct octahedral and tetrahedral environments seen in Ti-MCM-48G. In Figure 3d−f, spectra for 5, 10, and 18 atomic % Ti-grafted materials are shown. Each spectra is nearly identical with the exception of a slight broadening in the case of 18% Ti. As with Ti-MCM-48H, the two main peaks at 214 and 266 nm are assigned to titanium species in T_d and O_h coordination, respectively. The slight broadening observed could be the result of some Ti−O−Ti linkages formed during calcination.[34] The relative intensities ($I(O_h)/I(T_d)$) are consistently greater for the grafted materials than Ti-MCM-48H since all of the grafted Ti species are accessible to water ligation, owing to the preparative method. The spectrum of SBA-15 shown Figure 3a demonstrates the transparency of the unsubstituted siliceous materials throughout the UV−visible region.

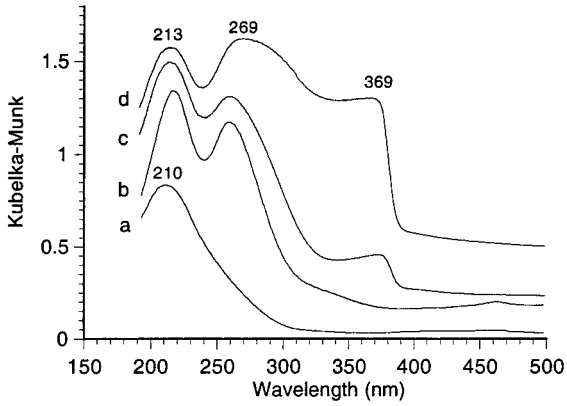

Figure 4. UV−visible spectra of the effect of water on the coordination sphere of titanium in TS-1 prepared by literature methods[6] run (a) dry and (b) moist; and Ti-MCM-48H run (c) dry and (d) moist.

Since each sample was run under ambient conditions, without dehydration, it can be inferred from inspection of main peak intensities that fewer Ti atoms in the hydrothermally prepared sample are initially six-coordinate compared to the grafted materials. The lower initial proportion of isolated titanium centers with an octahedral configuration in the hydrothermally prepared sample is to be expected for Ti sites within the silica matrix that are less accessible to water ligation. When the samples are moistened prior to analysis, the peak intensity of the O_h absorption increases at the cost of a decrease of the T_d peak as the Ti increases its coordination sphere with two additional water ligands (Figure 4c,d). Further evidence for this coordination sphere expansion is observed in TS-1 run as a moistened paste (Figure 4a,b). This reversible hydration effect and coordination sphere variability has been documented by Klein and co-workers for Ti/Si mixed oxide systems[33] and is likely responsible for the facile coordination of H_2O_2 and subsequent catalytic activity of Ti silicates.

Photoacoustic FTIR. Infrared spectroscopy yields valuable information concerning the framework of the support and the local titanium bonding environment in titanium containing mesoporous silicates. This technique has been successfully employed in the study of zeolite framework characteristics for over 30 years.[35] For modifications of the silicate framework and surface, MCM-48 provides an excellent fundamental spectrum as a basis for comparison since its peaks are clearly resolved. This point is illustrated in the comparison to the spectrum of amorphous silica (Figure 5). In the spectrum of MCM-48 there is a profound increase in peak resolution throughout the region ∼1300−600 cm^{-1} which can be ascribed to a degree of intermediate range order within the walls, which would be undetected by XRD.[36] The benefits of photoacoustic detection over transmission are made apparent when the sample is pelletized, pulverized, and rerun, showing a marked decrease in peak resolution and further confirming regions of intermediate range order within the silicate lattice (Figure 6).

The peak assignments of the pure silica MCM-48 (Figure 5A) can be made on the basis of early studies

(31) Bordiga, S.; Coluccia, S.; Lamberti, C.; Marchese, L.; Zecchina, A.; Boscherini, F.; Buffa, F.; Genoni, F.; Leofanti, G.; Petrini, G.; Vlaic, G. *J. Phys. Chem.* **1994**, *98*, 4125.

(32) Geobaldo, F.; Bordiga, S.; Zecchina, A.; Giamello, E.; Leofanti, G.; Petrini, G. *Catal. Lett.* **1992**, *16*, 109.

(33) Klein, S.; Weckhuysen, B. M.; Martens, J. A.; Maier, W. F.; Jacobs, P. A. *J. Catal.* **1996**, *163*, 489.

(34) Blasco, T.; Corma, A.; Navarro, M. T.; Pariente, J. P. *J. Catal.* **1995**, *156*, 65.

(35) Flanigen, E. M.; Khatami, H.; Szymanski, H. A. *Adv. Chem. Ser.* **1971**, *101*, 201.

(36) Flanigen, E. Personal communication.

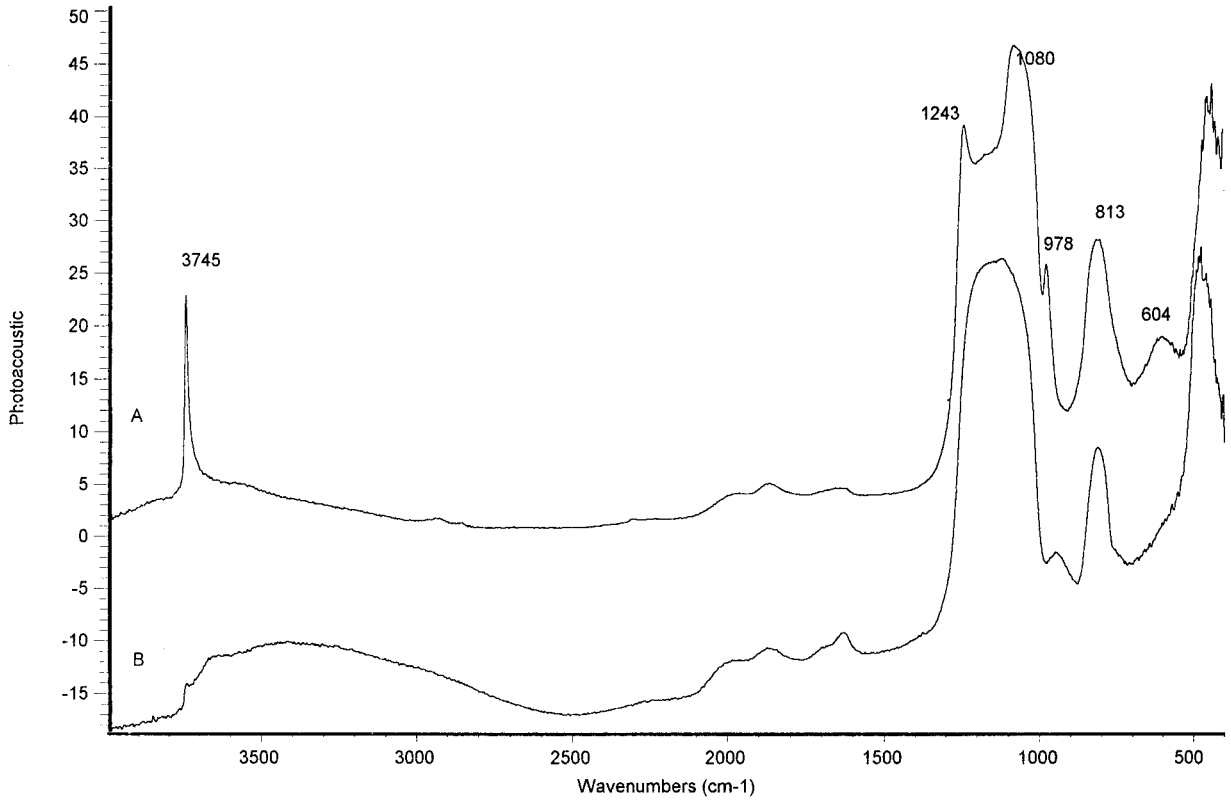

Figure 5. PAS-FTIR spectra of (a) pure silica MCM-48 and (b) Aerosil-600 amorphous silica.

on various silicates.[35] The sharp band at 3745 cm^{-1} assigned to isolated SiO−H stretches, is accompanied by a broad band from 3400 to 3700 cm^{-1} assigned to stretching frequencies of hydrogen bound silanols.[37] At lower frequencies, we observe three framework bands for the (Si−O−Si) ν_{as} at 1243 and 1083 cm^{-1} with a weak peak at about 1195 cm^{-1}. The strong peak at 817 cm^{-1} is attributed to (Si−O−Si) ν_{sym} while the band at 603 cm^{-1} could be ascribed to the "crystallinity peak" in zeolite synthesis, resulting from the formation of silica 5-rings during hydrothermal treatment.[38,39] The presence of this peak, which is notably absent in the spectrum of amorphous silica, is evidence for some intermediate range order within the walls. Associated with the silanol band at 3745 cm^{-1} is an absorption observed at 978 cm^{-1} which is assigned to the $Si-O^{\delta-}$ of a Si−OH stretch. The relative narrowness of this peak at 978 cm^{-1} can be explained by the contribution from the predominance of isolated silanols on the silica surface. When mesoporous silica is subjected to pressures exceeding 10 000 psi, the pores begin to undergo collapse. A sample of MCM-48 was crushed into a pellet following a procedure typical for the preparation of transmission IR samples to mimic the collapsed pore structure. Structural collapse was confirmed by XRD of the product. In the PAS-IR spectrum of crushed MCM-48 the loss in resolution in the range 1300−900 cm^{-1} can be clearly observed in Figure 6c. This proves unequivocally that the concerted (Si−O−Si) stretches that give rise to adsoprtion at 1243, 1195, and 1083 cm^{-1} are as a result of partial ordering of the silicate framework at the pore surface. Intermediate range ordering of this kind may therefore be promoted by the highly favorable electrostatic interactions between the cationic surfactant headgroup and the hydrolyzed anionic silica solution species prior to and during condensation and, additionally, extended hydrothermal treatment of MCM-48, allowing a more energetically favorable and narrower range of Si−O−Si bond angles. Collapse of the pores under excruciating pressure appears to eradicate this phenomenon.

Vibrations associated with the high surface density of isolated silanols, endemic to mesoporous silicates, experience profound change resulting from titanium incorporation by either route. As mentioned previously, removal of the surfactant during calcination generates surface silanols within the pores of MCM-48. The silanol surface density of ~1.4 OH/nm^2 roughly corresponds to the area mapped out by a surfactant headgroup in a hexagonal, close-packed array against the silica wall.[40] It was assumed that silanol density was roughly consistent between samples prepared with either surfactant and calcined under similar conditions. During grafting, these silanols react with the titanium isopropoxide precursor according to the following reaction:

$$(\equiv Si-OH)_x + Ti(iOPr)_4 \rightarrow (\equiv Si-O)_x-Ti(iOPr)_{4-x}$$

Since the formation of more than three Si−O−Ti linkages to the mesoporous walls would be sterically difficult to achieve, each Ti is expected to have at least one Ti−OH group resulting from the conversion of any remaining isopropoxy groups to titanols by calcination under

(37) Vansant, E. F.; Van Der Voort, P.; Vrancken, K. C. *Stud. Surf. Sci. Catal.* **1995**, *93*, 97.

(38) Jansen, J. C.; Van der Gaag, F. J.; Van Bekkum, H. *Zeolites* **1984**, *4*, 369.

(39) Zecchina, A.; Bordiga, S.; Spoto, G.; Marchese, L.; Petrini, G.; Leofanti, G.; Padovan, M. *J. Phys. Chem.* **1992**, *96*, 4985.

(40) Margolese, D. Ph.D. dissertation, University of California, Santa Barbara, 1995.

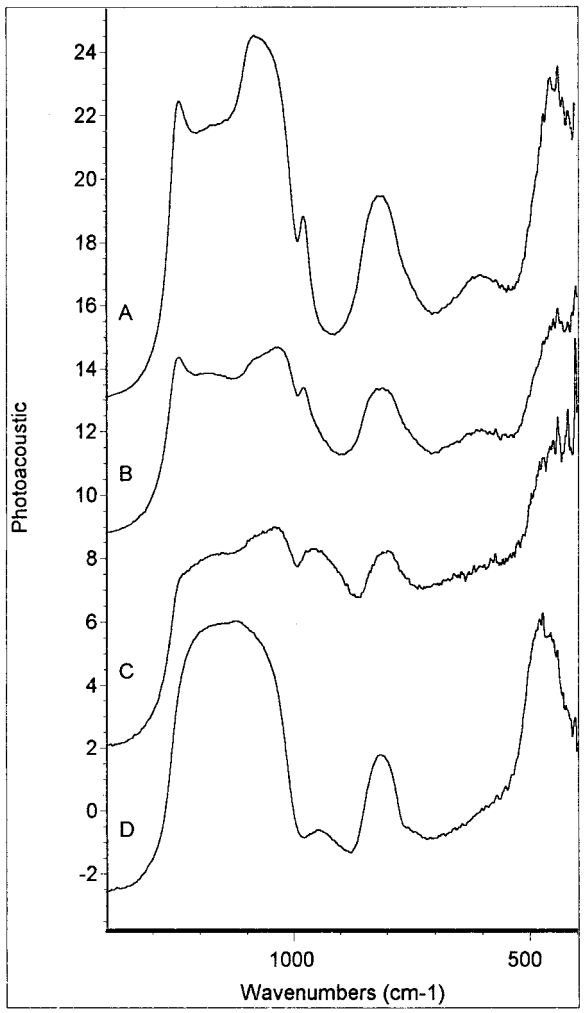

Figure 6. Low wavenumber (1400−400 cm^{-1}) range PAS-IR spectra of (a) MCM-48 prepared from CBDAC, (b) MCM-48 prepared from 18-12-18 (c) MCM-48 (from 18-12-18) following subjection to 12 000 psi, and (d) Aerosil-600 amorphous silica.

flowing oxygen. In Figure 7, we observe the appearance of a band in the high-frequency portion of the spectrum at 3675 cm^{-1} which can be readily assigned to the newly formed Ti−OH group.[41,42] Furthermore, a shoulder emerges at about 941 cm^{-1}, on the low energy side of the Si−OH stretch, which coalesces into a second peak with higher Ti content (Figure 8). The maximum of this peak at 930 cm^{-1} is more easily seen in the subtraction spectrum in (Figure 7c). In the titanium grafted MCM-48 sample, it is clear that absorptions due to surface silanol groups (3745−3500 and 978 cm^{-1}) are highly attenuated as a result of the formation of this new feature. At the highest loadings of titanium, a peak appears in the subtraction spectrum at 713 cm^{-1} which is the first signs of Ti−O−Ti bonds being formed between the more numerous titanium centers.[43]

A second and significant feature of the PAS-IR spectrum of Ti grafted MCM-48 is present within the region 980−930 cm^{-1} (Figure 7a), in which two distinct peaks can be observed at 978 and 930 cm^{-1}. Absorption in this region has been loosely attributed to the successful incorporation of titanium in crystalline and amorphous silicates, reported in the IR spectra of TS-1,[44] amorphous Ti/Si oxides,[45,46] Ti/Si aerogels,[47] and titanium grafted on amorphous silica.[48] The actual assignment of this peak is the source of ample controversy, since multiple species are believed to absorb in this frequency region, and the absorption is present in pure silica samples. Unfortunately, previous studies have failed to resolve the vibrations into more than one peak or shoulder. One species thought to be responsible for this band present in the IR spectrum of TS-1 is the titanyl (>Ti═O) group,[49] based on the appearance of absorptions in the region of 980−930 cm^{-1} for titanyl containing molecular species in solution.[50] An attempt to generate surface titanol species was made by grafting titanyl-containing precursors to the surface of silica under dry conditions, but its existence could not be demonstrated.[51] If it indeed could be isolated, the titanyl group would be immediately hydrolyzed into a more energetically stable (>$Ti(OH)_2$) as shown by density functional theory calculations.[51,52]

The remaining, most probable contributors to the 931 cm^{-1} absorption are either the perturbation of the Si−OH vibration by a neighboring titanium center[53] or the stretching of a newly formed, asymmetric Si−O−Ti bond. In titanasiloxanes, which possess only Ti−O−Si bonds and no silanol groups, an absorption is observed in this same region.[54] Additionally, Salvado et al. found that TiO_2−SiO_2 glasses had an absorption at 970 cm^{-1} that disappeared with heat treatment at 850 °C, giving rise to a new peak at 945 cm^{-1} that was unaffected by calcination.[55] In titanium silicalite samples,[56] the absorption observed at 962 cm^{-1} can be shifted to lower wavenumbers by ^{18}O-labeled water but not D_2O, unlike the peak at 985 cm^{-1} in pure silica.[57] On the basis of these two studies and the existence of two separate peaks at 978 and 930 cm^{-1} in our samples, it is unlikely that the lower energy absorption can be assigned to a shifted silanol. Furthermore, during grafting of titanium, some silanol groups remain unreacted, as seen by the residual peak at 3745 cm^{-1} for isolated silanols (Figures 7a and 8b−d). If we were to assume a range of

(41) Haukka, S.; Lakomaa, E. L.; Root, A. *J. Phys. Chem.* **1993**, *97*, 5085.
(42) Topsøe, N. Y. *J. Catal.* **1991**, *128*, 499.
(43) Villegas, M. A.; Depablos, A.; Fernandez-Navarro, J. M. *Glass Technol.* **1994**, *35*, 276.
(44) Perego, G.; Bellussi, G.; Corno, C.; Taramasso, M.; Buonomo, F.; Esposito, A. *Stud. Surf. Sci. Catal.* **1986**, *28*, 129.
(45) Klein, S.; Thorimbert, S.; Maier, W. F. *J. Catal.* **1996**, *163*, 476.
(46) Galan-Fereres, M.; Alemany, L. J.; Mariscal, R.; Banares, M. A.; Anderson, J. A.; Fierro, J. L. G. *Chem. Mater.* **1995**, *7*, 1342.
(47) Hutter, R.; Dutoit, D. C. M.; Mallat, T.; Schneider, M.; Baiker, A. *J. Chem. Soc., Chem. Commun.* **1995**, 163.
(48) Gao, X. T.; Bare, S. R.; Fierro, J. L. G.; Banares, M. A.; Wachs, I. E. *J. Phys. Chem. B* **1998**, *102*, 5653.
(49) Notari, B. *Stud. Surf. Sci. Catal.* **1987**, *37*, 413.
(50) Jeske, P.; Haselhorst, G.; Weyhermuller, T.; Wieghardt, K.; Nuber, B. *Inorg. Chem.* **1994**, *33*, 2462.
(51) Crocker, M.; Herold, R. H. M.; Roosenbrand, B. G.; Emeis, K. A.; Wilson, A. E. *Colloids Surf. A* **1998**, *139*, 351.
(52) Sinclair, P. E.; Sankar, G.; Catlow, C. R. A.; Thomas, J. M.; Maschmeyer, T. *J. Phys. Chem. B* **1997**, *101*, 4232.
(53) Scarano, D.; Zecchina, A.; Bordiga, S.; Geobaldo, F.; Spoto, G.; Petrini, G.; Leofanti, G.; Padovan, M.; Tozzola, G. *J. Chem. Soc., Faraday Trans.* **1993**, *89*, 4123.
(54) Voigt, A.; Murugavel, R.; Chandrasekhar, V.; Winkhofer, N.; Roesky, H. W.; Schmidt, H. G.; Uson, I. *Organometallics* **1996**, *15*, 1610.
(55) Salvado, I. M. M.; Navarro, J. M. F. *J. Non-Cryst. Solids* **1992**, *147*, 256.
(56) Bellussi, G.; Carati, A.; Clerici, M. G.; Maddinelli, G.; Millini, R. *J. Catal.* **1992**, *133*, 220.
(57) Boccuzzi, F.; Coluccia, S.; Ghiotti, G.; Monterra, C.; Zecchina, A. *J. Phys. Chem.* **1978**, *82*, 1298.

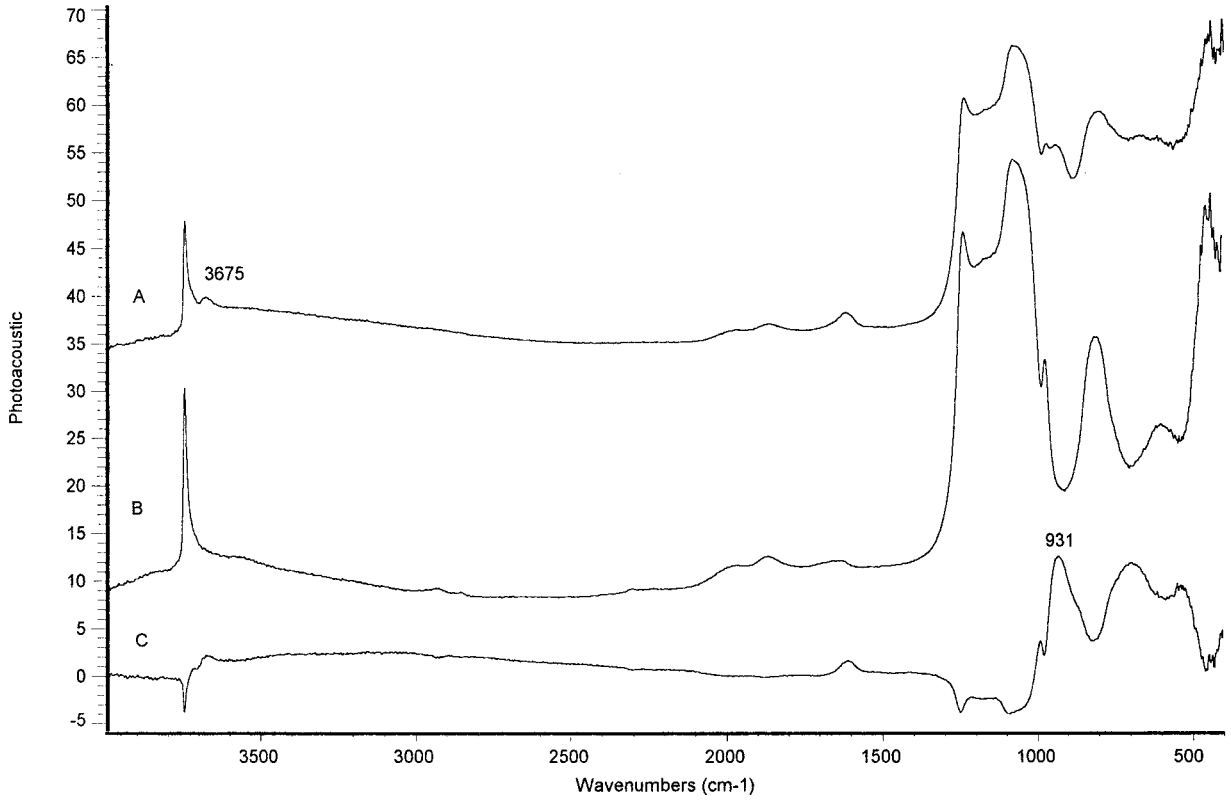

Figure 7. PAS-FTIR spectra of (a) 17.5 atomic % grafted titanium on (b) pure silica MCM-48 support with (c) subtraction spectrum.

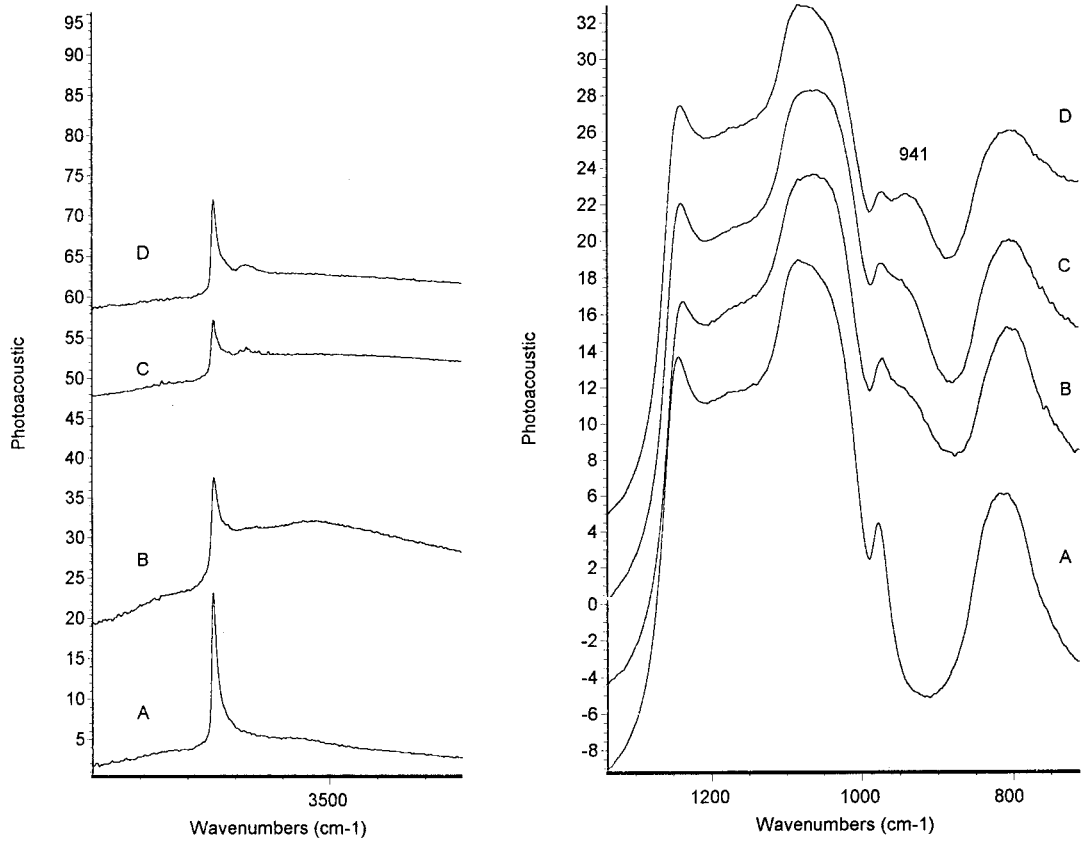

Figure 8. PAS-FTIR spectra of MO−H and framework region for the pure silica MCM-48 support and subsequent higher Ti loadings: (a) MCM-48, (b) 5% grafted Ti, (c) 10% Ti, and (d) 17.5% Ti.

distances and hence influences on the Si−OH vibration by a neighboring titanium center, we would expect to see the peak at 978 cm^{-1} simply shifted to a lower frequency and broadened. Instead, since we were able to resolve two peaks between 980 and 930 cm^{-1}, it is clear that more than one species is responsible for absorptions in this region, with the second peak being assigned to the vibration of asymmetric $Si-O^{\delta-}-Ti^{\delta+}$

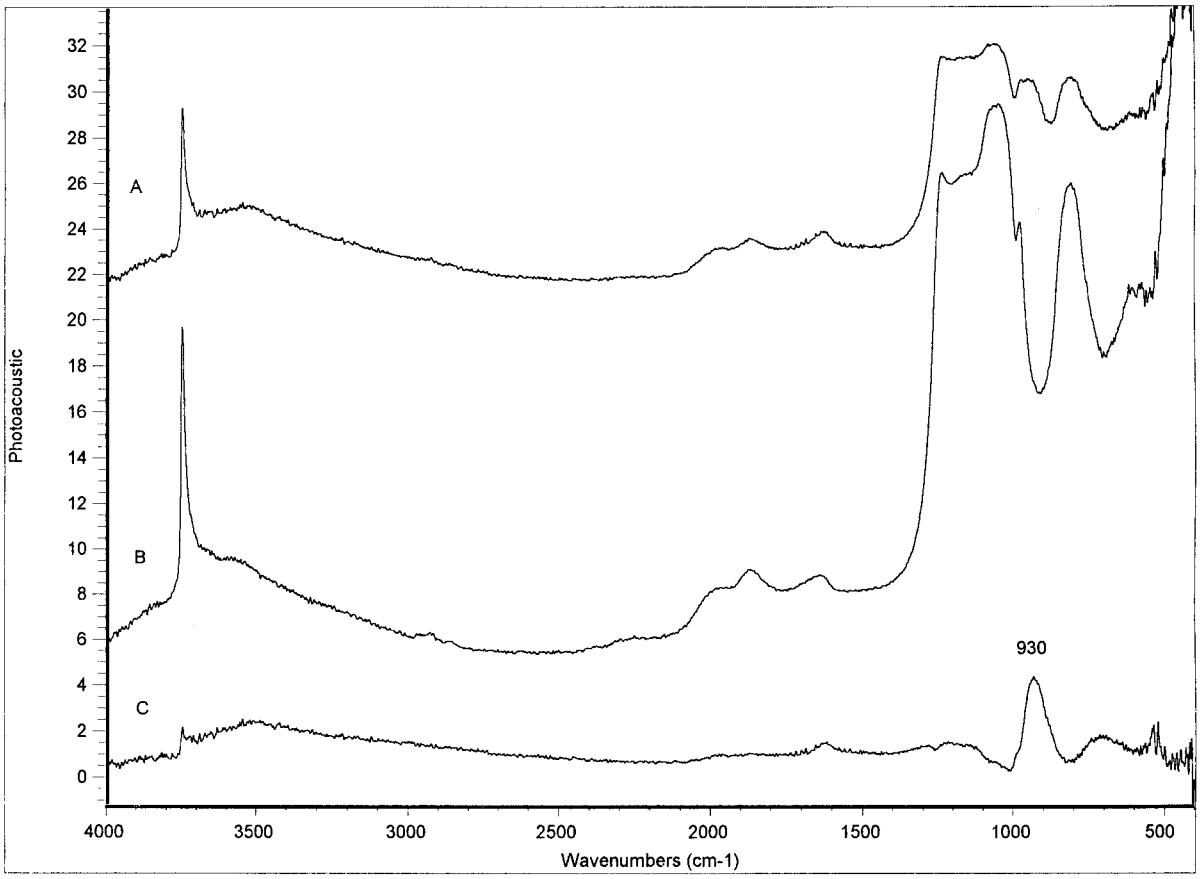

Figure 9. PAS-FTIR spectra of (a) Ti−MCM48 prepared with 18-12-18, (b) pure silica MCM-48, and (c) subtraction spectrum.

bonds. In our case, the peak is shifted to a lower frequency from the expected 960 cm^{-1}, indicating possible longer, strained oxygen bridges to the titanium centers.

Incorporation of titanium into MCM-48 by hydrothermal methods exhibits similar absorbances to the grafted samples in the PAS-FTIR spectra (Figure 9). The main difference is that in the Ti-MCM-48H sample, the TiO−H stretch is too weak to be differentiated from the noise, indicating a low or negligible abundance. The absence of this signal is likely a result of Ti ions being embedded within the walls surrounded by four silicate tetrahedra as opposed to existing primarily on the surface. In the framework region of the subtraction spectrum (1300−600 cm^{-1}), a new peak is seen again at 930 cm^{-1} for the Ti containing sample and is attributed to a Ti−O−Si bond. Furthermore, in the hydrothermally prepared sample as well as the grafted samples, the bending mode frequency of physisorbed water shifts to a lower frequency. On the pure silica MCM-48 sample, the H−O−H bending occurs between 1655 and 1640 cm^{-1} (Figure 5a). When Ti is introduced by grafting (Figure 7a) and hydrothermal techniques (Figure 9a) the new vibration seen in the subtraction spectra is shifted to 1610−1616 cm^{-1}. This shift can be compared to the water bending vibration occurring on pure TiO_2 of 1646 cm^{-1} and effectively shows that water exhibits stronger coordination to the metal centers in Ti/MCM-48 materials than to either pure silica or titania.

The PAS−FTIR spectra of SBA-15 and Ti−SBA-15G (Figure 10) exhibit similar overall characteristics to that of siliceous and Ti grafted MCM-48 respectively, however some differences between the host materials and the result of grafting are apparent. In the IR spectrum of SBA-15 (Figure 10b) the presence of isolated silanol groups is clearly indicated by the (SiO−H) adsorption at 3745 cm^{-1}, which is subsequently entirely lost upon grafting of titanium isopropoxide. In the lower frequency range of the IR spectrum, the adsorption bands associated with the silicate frameworks of MCM-48 and SBA-15 demonstrate a differing spectral profile. The lack of adsorption at 1250−1200 cm^{-1} above the background and a weaker adsorption at 1080 cm^{-1} suggests that SBA-15 has a broader distribution of (Si−O−Si) ν_{as} frequencies than MCM-48. As previously mentioned, no significant adsorption at ∼600 cm^{-1} relating to intermediate range order within the silicate walls was observed. The appearance of this spectral region could be described as being between that of MCM-48 and amorphous silica (Figure 5), and suggests that less (if any) intermediate range order is evident in SBA-15. The lower temperature synthesis route to the product and the thicker walls present in SBA-15 (30−60 Å, determined from TEM)[4] support the notion of a more amorphous framework compared to MCM-48. The IR spectrum of Ti-SBA-15G (Figure 10a**)** is lacking in substantial characteristic TiO−H adsorption at 3675 cm^{-1}, yet there is an increase in adsorption in the range 980−930 cm^{-1} (notable in the subtraction, Figure 10c), attributed to successful incorporation of Ti into the silicate matrix. Furthermore, in the subtraction spectrum, a broad band centered at 700 cm^{-1} can be attibuted to the presence of Ti−O−Ti bonds.

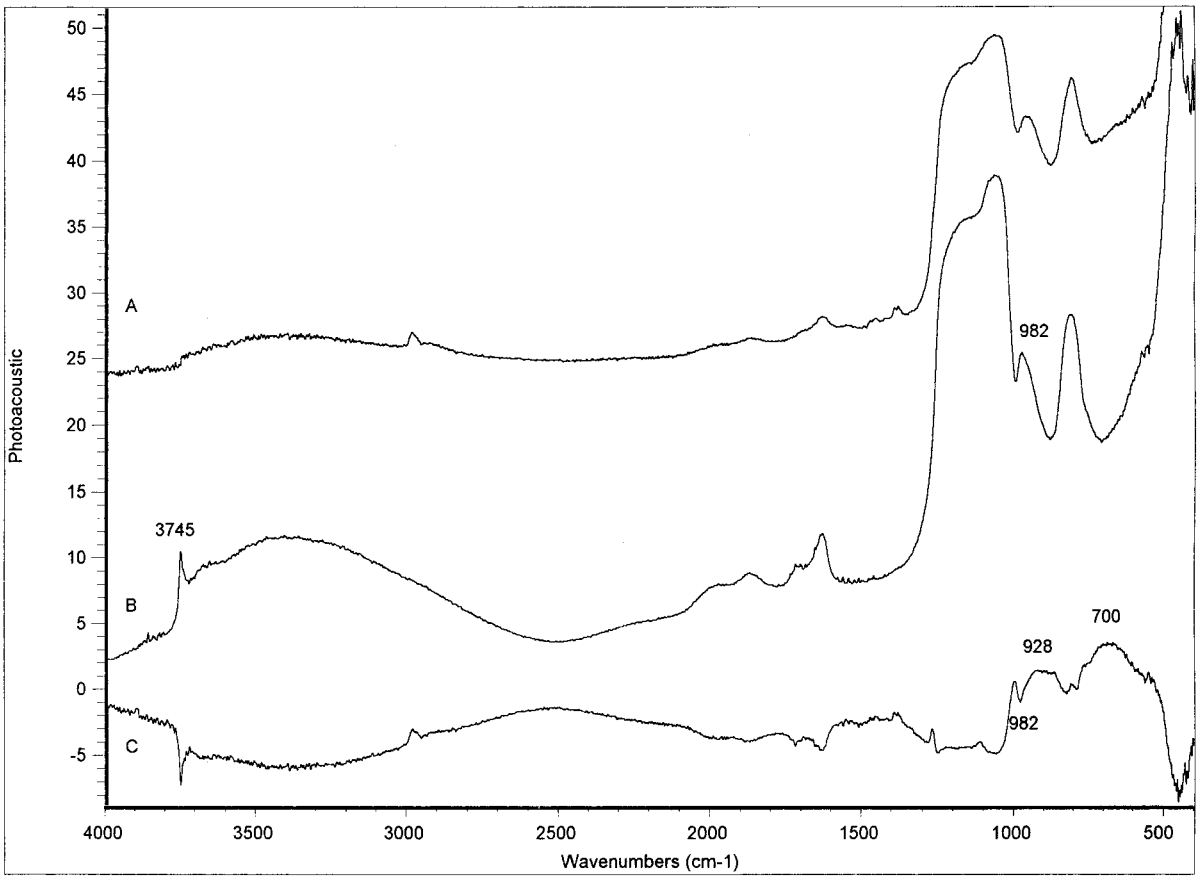

Figure 10. PAS-FTIR spectra of (a) Ti-SBA-15G, (b) SBA-15, and (c) subtraction spectrum.

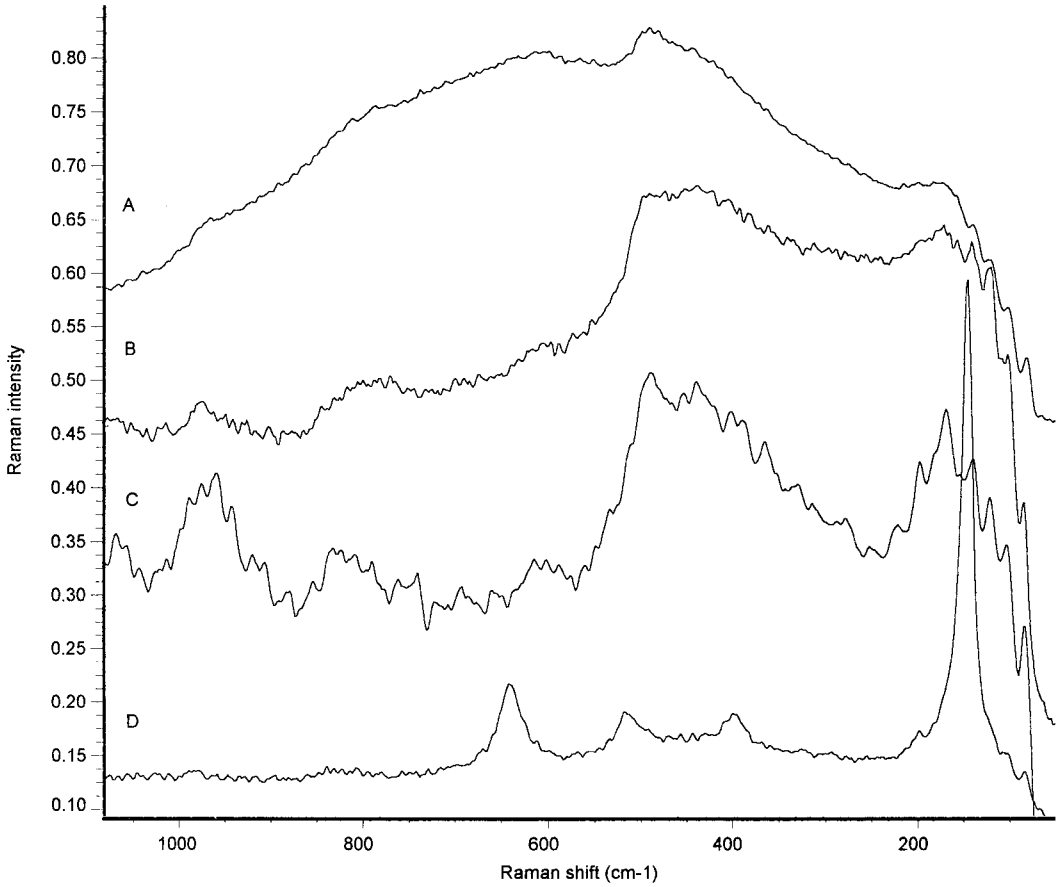

Figure 11. Raman spectra of titanium grafted at (a) 17.5 atomic % Ti, (b) 5 atomic % Ti, and (c) hydrothermally prepared Ti-MCM48 versus (d) a mechanical mixture of 5% anatase and calcined MCM-48.

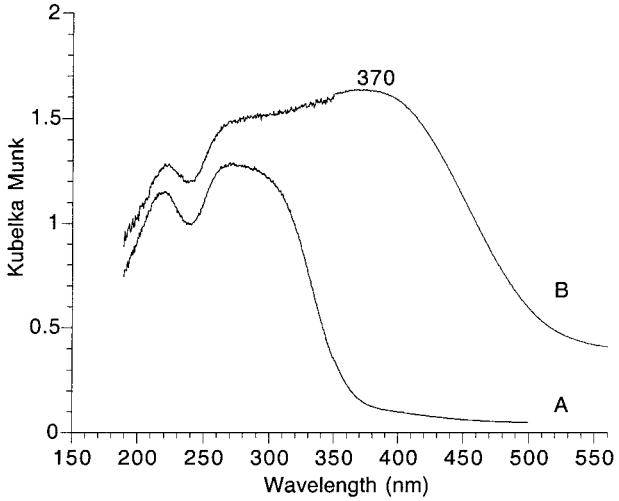

Figure 12. UV−visible spectra of (a) 5% Ti grafted and the (b) yellow product after contact with H_2O_2.

Raman Spectroscopy. Raman spectroscopy has been used effectively to determine the absence of bulk titania since it is sensitive to the easily polarized Ti−O bond. In Figure 11d, Raman spectra for a mechanical mix of 5% TiO_2/SiO_2 featuring absorbances at 638, 514, 394, and 144 cm^{-1} characteristic of the anatase phase[58] are shown. In both Ti−MCM-48 (Figure 11c) and grafted samples including the XS loaded sample (Figure 11a,b), no sign of the most intense absorbance at 144 cm^{-1} can be observed, confirming the absence of extraframework, bulk crystalline titania. Raman has been found to work best for crystalline oxides. Amorphous oxides have a wide distribution of bond angles, leading to a broadening of peaks and a more featureless signal. Although TiO_2 was detected in the Ti-MCM-48H sample by UV−vis, it is likely amorphous and not as easily recorded by Raman.

Interaction with Hydrogen Peroxide. Given the exceptional performance of Ti-grafted MCM-48 toward the halogenation of large organic dye molecules in the presence of H_2O_2,[19] we investigated the intermediates formed with the oxidant by multiple spectroscopic techniques. When the titanium containing samples prepared by either method are contacted with aqueous solutions of hydrogen peroxide, the solids turn yellow due to the formation of stable Ti−OOH intermediates. Once formed, these intermediate species are stable to drying and maintain their yellow tint for many months.[59] While both types of Ti incorporated MCM-48 undergo this coordinative modification by peroxide, the grafted samples are visibly more affected. We found that approximately twice the amount of peroxide molecules were coordinated per titanium atom in Ti-MCM-48G versus Ti-MCM-48H.[60] While not quantified, it can be assumed that the number of Ti−OOH groups per total titanium content to be lower for the hydrothermally prepared material since many Ti centers within the walls could be inaccessible to peroxide coordination. These intermediates were then studied by the same spectroscopic techniques described previously to add insight into their formation, stability, and reactivity.

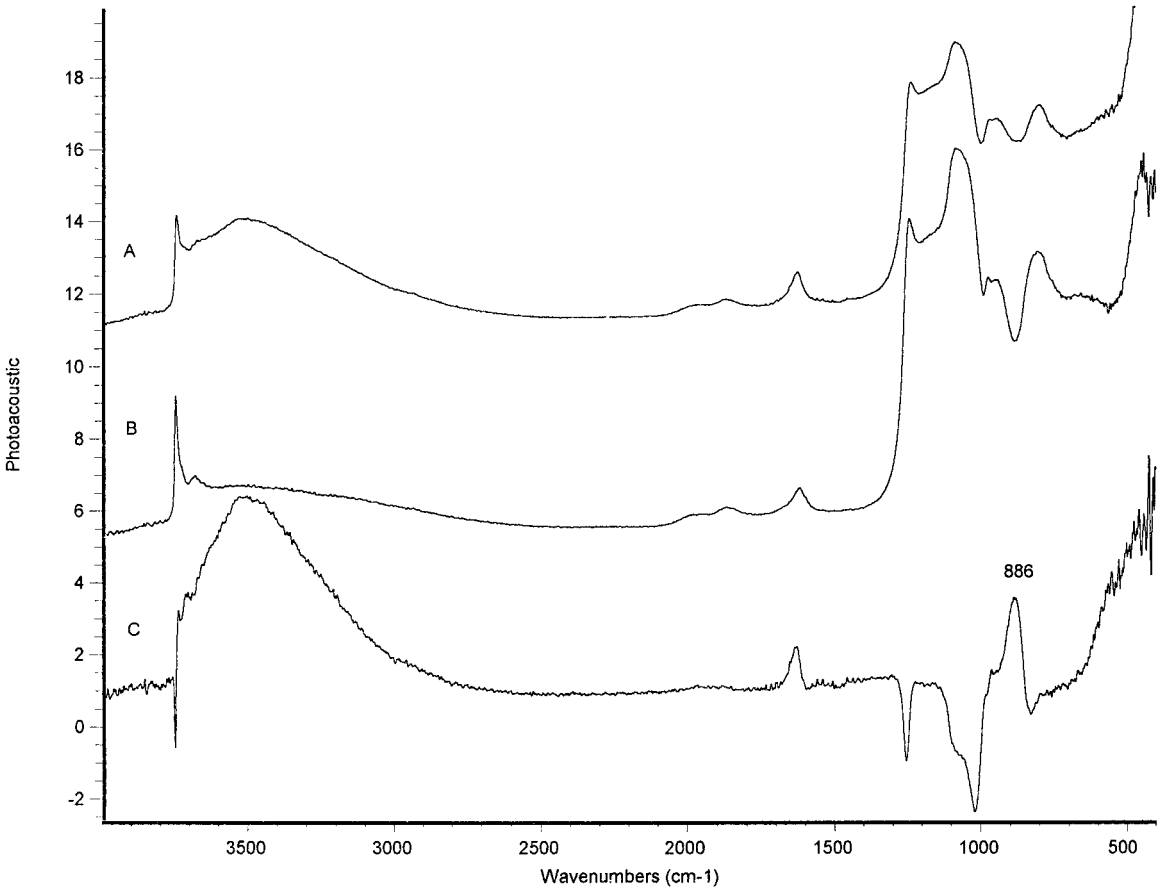

Figure 13. PAS-FTIR spectra of (a) 10 atomic % Ti grafted contacted with H_2O_2 and then dried, (b) original 10 atomic % Ti grafted sample, and (c) the subtraction spectrum (expanded).

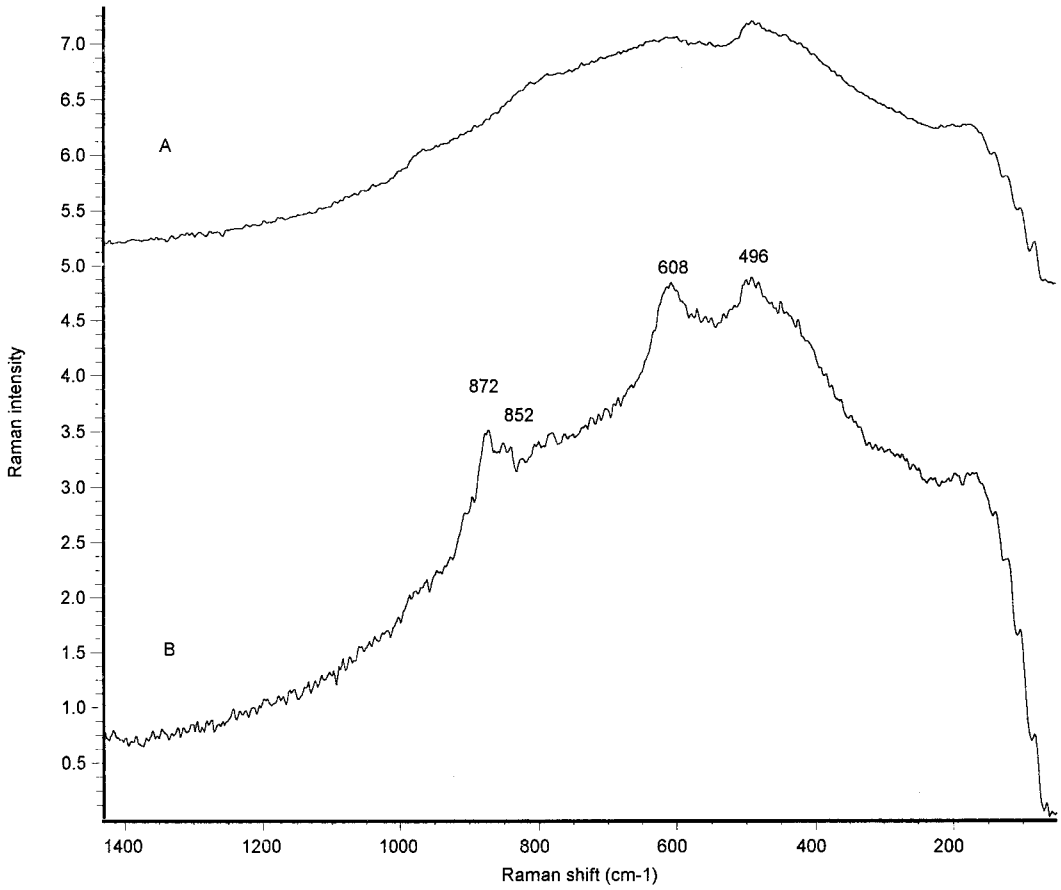

Figure 14. Raman spectra of (a) 17.5 atomic % Ti grafted on pure silica MCM-48 and (b) sample run as a slurry with dilute (~1%) H_2O_2.

The origin of the yellow color of titanium−peroxy species can best be illustrated with UV−visible spectroscopy, where the ligand to metal charge-transfer band absorption can be seen red shifting into the visible region (Figure 12). Hydrogen peroxide adsorbed on TiO_2 gives a strong peak at 400 nm with a weak shoulder at 455 nm in the UV−visible spectrum corresponding to a $\sigma \rightarrow \sigma^*$ and $\pi \rightarrow \sigma^*$ transition for a peroxide bound "side-on" and "end-on" as hydroperoxide, respectively.[61] For the 5% Ti grafted on MCM-48, a broad peak arises upon contact with dilute H_2O_2 which has a maximum at about 370 nm and gradually tapers off toward longer wavelengths. Although the weak shoulder at 455 nm cannot be resolved, it is likely from the blue shift of the peak maximum that the predominant species is peroxide bound "side-on". From our previous catalytic tests,[19] this absorption vanished after the catalyzed bromination reaction, illustrating the integral yet transitory nature of this Ti−OOH intermediate.

After establishing the existence of coordinated peroxide on titanium centers contained in MCM-48, we employed PAS-FTIR and Raman to elaborate on the change in the vibrational strength of the O−O peroxy bond. In an early study, Mühlebach et al.[62] synthesized a number of titanium peroxo salts and found them to have peroxo vibrations between 800 and 1000 cm^{-1}. In the PAS-FTIR spectra of 10% Ti grafted on MCM-48 contacted with H_2O_2 (Figure 13), a new peak arises at 886 cm^{-1} which is readily assigned to the O−O stretch of a bound peroxo group. The effect of peroxide coordination to a titanium center on the strength of the O−O bond was further studied in situ with Raman spectroscopy (Figure 14).[63] The sample was placed in a quartz capillary and slurried with dilute H_2O_2. This provides a cooling effect and prevented burning of the sample by the probe laser. Upon immersion in the peroxide solution, the sample effervesced, indicating the decomposition of the peroxide species to form oxygen gas. This decomposition led to a decrease in the intensity of the peak at 852 cm^{-1}, which can thus be assigned to bound peroxide. The poor signal-to-noise ratio is a result of the fewer than normal number of scans that could be collected and Fourier transformed before the total disappearance of the peroxo stretch. The lower frequency position of this peak relative to that of unbound, aqueous H_2O_2 at 872 cm^{-1} is evidence for the weakening of the O−O bond and is the key to the catalytic activity of titanium silicates in the presence of a peroxide source.

(58) Pilz, W.; Peuker, C.; Tuan, V. A.; Fricke, R.; Kosslick, H. *Int. J. Phys. Chem.* **1993**, *97*, 1037.
(59) Kubota, L. T.; Gushikem, Y.; Mansanares, A. M.; Vargas, H. *J. Colloid. Interface Sci.* **1995**, *173*, 372.
(60) Morey, M.; Carlsson, H.; Walker, J.; Buttler, A.; Stucky, G. D. Unpublished results.
(61) Klissurski, D.; Hadjiivanov, K.; Kantcheva, M.; Gyurova, L. *J. Chem. Soc., Faraday Trans.* **1990**, *86*, 385.
(62) Mühlebach, J.; Müller, K.; Schwarzenbach, G. *Inorg. Chem.* **1970**, *9*, 2381.
(63) Tengvall, P.; Vikinge, T. P.; Lundstrom, I.; Liedberg, B. *J. Colloid. Interface Sci.* **1993**, *160*, 10.

Conclusions

A simple and effective synthetic method for the incorporation of titanium centers into mesoporous silica has been devised and described. Hydrothermal and postsynthesis grafting methods yielded high surface area (600−1300 m^2/g) highly ordered mesoporous supports, MCM-48 and SBA-15, containing isolated and catalytically active titanium sites. The three-dimensional pore array of MCM-48 and the ultralarge pores of SBA-15 provide unique morphologies of potential utility in the catalysis of large substrates, compared to alternative high surface area supports. The materials are also highly thermally stable (>800 °C) and resist structural degradation after extended periods in water. Using a combination of molecular analytical techniques, we have unveiled the structural nature and local titanium environments of these unique materials. In the case of Ti-MCM-48 we have established that more than one species contributes to the absorbance at 960 cm^{-1}, and stable Ti−peroxo intermediates were observed. Photoacoustic (PAS) FTIR proved a substantial advancement over conventional transmission FTIR spectroscopic characterization of both the host materials and the titanium incorporated catalysts, due to the nondestructive nature of sample analysis, which leads to significantly improved resolution. PAS-FTIR provided evidence that extended hydrothermal treatment of MCM-48 leads to regions of intermediate range order within the walls, which is neither observed in amorphous silica nor SBA-15.

As with all mixed-oxide heterogeneous catalysts, surface accessibility of active sites to passing substrates is an integral part of their reactivity. To maximize this parameter and hence reactivity, metal centers must be isolated and exist on or near the surface of a durable, high surface area material. It has been demonstrated that using MCM-48 and SBA-15 as supports for titanium grafting enhances these desired properties by producing predominantly isolated surface species and avoiding metal oxide cluster formation or support degradation. On the other hand, in hydrothermally prepared Ti-MCM-48H, many of the titanium species may be encapsulated within the walls and inaccessible for catalysis. For catalytic applications, a grafted support would be recommended over hydrothermally prepared materials due to wider range of heteroatom loadings possible and greater relative ease in synthesis. Of the two supports studied, MCM-48 had higher possible Ti loadings than SBA-15, but has a smaller pore aperture. Since SBA-15 is still an interesting and unexplored large-pore silica support, future studies are needed to optimize surface functionality for specialized applications.

Acknowledgment. We gratefully acknowledge the NSF for funding under award DMR-9520971. This work made use of the MRL Central Facilities supported by the National Science Foundation under Award No. DMR96-32716. M. Morey wishes to thank Wayne Lukens, Anne Davidson and Ellie Fairbairn for helpful suggestions. S. O'Brien thanks the Lindemann Trust Fellowship Fund.

CM9901663